Pergamon

PII: S0277-5387(97)00079-X

Polyhedron Vol. 16, No. 19, pp. 3293–3304, 1997

0277-5387/97 $17.00+0.00

An NMR and single-crystal X-ray diffraction structural study of Ru^{II} [12]aneS_4 polypyridyl complexes

Brian J. Goodfellow,[a,c]* Sara M. D. Pacheco,[a] Julio Pedrosa de Jesus,[a] Vitor Félix[a,d]* and Michael G. B. Drew[b]*

[a] Departamento de Química, Universidade de Aveiro, 3800 Aveiro, Portugal

[b] Department of Chemistry, The University, Whiteknights, Reading RG6 6AD, U.K.

[c] Departamento de Química e Centro de Química Fina e Biotecnologia, Faculdade de Ciências e Tecnologia, Universidade Nova de Lisboa, 2825 Monte de Caparica, Portugal

[d] Instituto de Tecnologia Química e Biológica, Rua da Quinta Grande 6, 2780 Oeiras, Portugal

(Received 18 December 1996; accepted 13 February 1997)

Abstract—The synthesis of a series of Ru^{II} complexes with the thioether ligand [12]aneS_4 (1,4,7,10-tetrathiocyclododecane) and various polypyridyl ligands was carried out using $[Ru(DMSO)_4Cl_2]$ (DMSO- = dimethylsulphoxide) as a starting material. The first synthetic step involved the introduction of the thioether ligand and the isolation of the compound $[Ru([12]aneS_4)Cl_2]$. The polypyridyl ligands were then exchanged to give a series of complexes $[Ru([12]aneS_4)(X)]^{2+}$ [X = 1,10 phenanthroline (phen), 2,2′-bipyridyl (bpy) and 4,7′-diphenyl-1,10-phenanthroline (dip)]. Crystal structures of the metal complexes $[Ru([12]aneS_4)(bpy)]Cl_2 \cdot 4H_2O$, $[Ru([12]aneS_4)(phen)]Cl_2 \cdot 4.25H_2O$ and $[Ru([12]aneS_4)(dip)]Cl_2 \cdot 2H_2O$ all show the Ru centre in a distorted *cis*-octahedral environment, in which the equatorial coordination plane is formed by two S-donor atoms of the macrocyclic ligand [12]aneS_4 and two N-donor atoms of a polypyridyl ligand: bpy, phen or dip. The hexa coordination is completed *via* the remaining sulfur atoms of the macrocycle. The distortion of the octahedral geometry is associated with the small cavity size of macrocyclic ligand and small bite angle of the bidentate polypyridyl ligands [77.9(3)° bpy, 79.6(3) phen and 77.4(4)° dip]. The small cavity size of [12]aneS_4 precludes the sulfur atoms of the macrocycle achieving axial positions of an ideal octahedron leading to angles, S_{ax}—Ru—S_{ax}, of 162.5(2), 161.9(1) and 162.0(1)° for the bpy, phen and dip complexes respectively. A ^1H and ^{13}C NMR study of the complexes $[Ru([12]aneS_4)(phen)]^{2+}$, $[Ru([12]aneS_4)(bpy)]^{2+}$ and $[Ru([12]aneS_4)(dip)]^{2+}$ was carried out. The ^1H spectra exhibit broad lines for the H-2 and H-9 protons of the polypyridyl ligand and the CH_2 protons of the [12]aneS_4 ligand. A variable temperature study indicated that exchange processes were taking place in solution, most probably involving cleavage of the Ru—N bond as a result of the strain on the octahedral environment of the small cavity size of the [12]aneS_4 macrocycle. © 1997 Elsevier Science Ltd

Keywords: 1,4,7,10-tetrathiacyclodecane ruthenium complexes; single-crystal X-ray diffraction; NMR spectroscopy.

Since the early 1980s when Barton *et al.* [1] studied the interaction of the two isomers of $[Ru(1,10\text{-phenanthroline})_2Cl_2]$ with B-DNA the area of transition metal–DNA interactions has seen much work. DNA has been found to interact with transition metal complexes in a variety of ways including intercalation, whereby a polypyridyl ligand of the transition metal complex is inserted (fully or partially) between the stacked bases of the DNA double helix, surface binding, within one of the DNA grooves, and covalent binding where ligands in the Ru complex are replaced by heteroatoms of the DNA bases (normally the nitrogen of guanine) [1–12].

The use of transition metal complexes as anti-tumour agents, following the work of Rosenberg *et*

* Authors to whom correspondence should be addressed.

al. [13] in 1969 with *cis*-platin, has expanded to include the whole of the platinum group metals. In the last few years, Alessio *et al.* [14] found that *trans*-$[Ru(DMSO)_4Cl_4]$ showed promising anti-tumour activity with adjacent guanines being the preferred interaction site on DNA, while Keppler *et al.* [15] carried out an extensive study of various Ru complexes, finding that $[Ru(Im)_2Cl_4]$ (ImH) and $[Ru(Ind)_2Cl_4]$ (IndH), where Im = imidazole and Ind = indazole, show anti-tumour activity.

These *in vitro* studies of Ru complexes have shown that the number and type of polypyridyl, and ancillary, ligands have a profound effect on the manner and type of interaction with biomolecules. Factors such as the ability of the ligands to form hydrogen bonds or favourable VDW interactions with the functional groups of the DNA bases have been found to play a determining role in binding. A first step in the design of Ru complexes with selective DNA binding characteristics is the choice of a suitable ligand followed by the structural characterization of the complex.

The use of macrocyclic polyamines and polythioethers in transition-metal chemistry has been considerable as these ligands are thermodynamically and kinetically inert and also have the ability to stabilize unusual oxidation states (e.g. Rh^{II}) [16]. For ruthenium, macrocycle ligands such as [9]aneS_3 and [12]aneS_4 bind strongly and are not easily substituted allowing facile substitution of the remaining ligands. They also stabilize the Ru^{II} oxidation state which is diamagnetic allowing high-resolution NMR experiments to be performed. Krotz *et al.* [17] synthesized a series of Rh^{III} complexes with cyclic polyamines or [12]aneS_4 and a 9,10-diaminophenanthrene ligand in order to probe specific binding interactions to DNA.

A systematic variation of thioether–polypyridyl ligands complexed to Ru^{II} allows conclusions to be drawn as to the structural characteristics of these compounds and the role these play in DNA binding, the goal being the design of a complex with specific DNA binding characteristics. The first step in this process is, therefore, the synthesis and characterization of the Ru^{II}-based complexes followed by the determination of their three-dimensional structure.

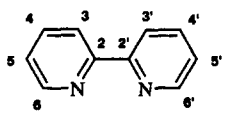

bpy

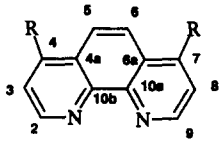

R=H phen
R=Ph dip

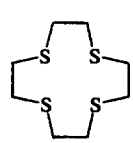

[12]aneS_4

Scheme. 1.

In this paper the synthesis (from $[Ru(DMSO)_4Cl_2]$) of a number of $[Ru([12]aneS_4)(X)]$ complexes [X = 1,10 phenanthroline (phen), 2,2′-bipyridyl (bpy), 4,4′-diphenyl-2,2′-bipyridyl (dbp) and 4,7′-diphenyl-1,10-phenanthroline (dip)] is reported along with their spectroscopic characterization. The structures of $[Ru([12]aneS_4)(phen)]^{2+}$, $[Ru([12]aneS_4)(bpy)]^{2+}$ and $[Ru([12]aneS_4)(dip)]^{2+}$ are compared in solution by NMR and in the solid state by X-ray crystallography.

EXPERIMENTAL

The ligands [12]aneS_4, phen, bpy and dip were purchased from the Aldrich Chemical Company and used without further purification.

Syntheses

$[Ru(DMSO)_4Cl_2]$. The synthesis of $[Ru(DMSO)_4Cl_2]$ was carried out according to the method of Evans *et al.* [18].

$[Ru([12]aneS_4)Cl_2]$. $[Ru(DMSO)_4Cl_2]$ (0.5 g, 1.03 mmol) was added to 0.186 g of [12]aneS_4 (0.78 mmol) in ethanol (*ca* 30 cm^3). The resulting suspension was refluxed for 90 min at 80°C. A colour change from pale to bright yellow indicated reaction. The solution was concentrated and a bright yellow solid obtained. The product was washed with ethanol and dried (0.39 g, 92%). NMR: ^1H D_2O; 3.95 m, 3.45 m, 3.20 m, 2.71 m 16 H, [12]aneS_4; ^{13}C 46.6, 45.0, 41.4, 40.5, 33.6 and 33.1 (all ppm).

$[Ru([12]aneS_4)(2,2'\text{-bipyridyl})]Cl_2$ (**1**). A 2% excess of 2,2′-bipyridyl (0.097 g, 0.621 mmol) was added to 0.250 g of $[Ru([12]aneS_4)Cl_2]$ (0.25 g, 0.606 mmol) in ethanol. The yellow solution was refluxed for 2.5 h at 80°C and an orange/red solution obtained. The solution was concentrated to dryness and redissolved in $EtOH/H_2O$. On standing large orange/red crystals were obtained (0.23 g, 67%). Found: C, 32.6; H, 5.5; N, 3.9. Calc. for $[Ru([12]aneS_4)(bpy)]Cl_2 \cdot 4H_2O$; C, 33.7; H, 4.9; N, 4.4%. NMR: ^1H CD_3OD (298 K); {9.460 br 2H, 8.743 d 2H, 8.264 dd 2H, 7.776 dd 2H} bpy; {3.839 br, 3.620 br, 3.026 br 16H} [12]aneS_4; ^{13}C {158.4, 151.7 br, 139.9, 127.7, 125.7} (bpy), {44.9 br, 35.4 br} [12]aneS_4.

$[Ru([12]aneS_4)(1,10\text{-phenanthroline})]Cl_2$ (**2**). 1,10-Phenanthroline (0.108 g, 0.546 mmol, 5% excess) was added to a solution of $[Ru([12]aneS_4)Cl_2]$ (0.236 g, 0.981 mmol) in ethanol. The yellow solution was refluxed for 2 h at 80°C until an orange precipitate appeared. The solution was concentrated until a solid was obtained. On standing, small orange crystals

developed. These were washed with water and dried (0.5 g, 94%). Found: C, 34.3; H, 5.0; N, 3.9. Calc. for $[Ru([12]aneS_4)(phen)]Cl_2 \cdot 4.25H_2O$: C, 35.9; H, 4.9; N, 4.1%. NMR: ^1H CD_3OD (298 K); {9.821 s br 2H, (8.861, 8.857, 8.834, 8.829) dd 2H, 8.309 s 2H, (8.133, 8.114, 8.105, 8.087) dd 2H} phen, {3.876 br, 3.690 br, 3.178 br 16H} [12]aneS$_4$. ^{13}C {152.4 br, 148.7, 139.3, 132.8, 129.1, 126.2} (phen), {45.0 br, 35.9 br} [12]aneS$_4$.

$[Ru([12]aneS_4)(4,7'\text{-diphenyl-1,10-phenanthroline})]Cl_2$ (**3**). To the complex $[Ru([12]aneS_4)Cl_2]$ (0.132 g, 0.320 mmol) in ethanol was added to 0.108 g (0.325 mmol) of 4,7′-diphenyl-1,10-phenanthroline. After refluxing for 2.5 h at 80°C a red/orange solution was obtained. Concentration of the solution yielded a red solid (0.12 g, 50%). Found: C, 51.6; H, 4.8; N, 3.7. Calc. for $[Ru([12]aneS_4)(dip)]Cl_2 \cdot 2H_2O$: C, 49.2; H, 4.6; N, 3.7%. NMR: ^1H CD_3OD (298 K); {9.910 br 2H, 8.213 s 2H, 8.080 d 2H, 7.711–7.651 m 10H} dip, {3.906 br, 3.751 br, 3.217 br 16H} [12]aneS$_4$. ^{13}C {152.1 br, 151.9, 149.6, 137.3, 131.2, 130.7, 130.6, 127.1, 126.8 br} (dip), {45.4 and 36.3} ([12]aneS$_4$).

Single-crystal structure determination

The crystal data and structure refinement details are given in Table 1. Data for all three complexes were collected with a MARresearch image plate system using graphite-monochromated Mo-K_α radiation ($\alpha = 0.71073$ Å). The crystals were positioned 75 mm from the image plate. An exposure time of 2 min was used per 2 frames collected. Data analysis was carried out with the XDS program [19]. Intensities were not corrected for absorption effects.

The positions of the ruthenium atoms were obtained from three-dimensional Patterson maps and the remaining non-hydrogen atoms positions by successive difference-Fourier synthesis. After the anisotropic refinement of $[Ru([12]aneS_4)(phen)]Cl_2 \cdot 4.25H_2O$, a Fourier-difference map showed an isolated peak with an electronic density of 1.50 e A^{-3}, which was assigned to an oxygen of a water of crystallization with an occupation factor of 0.25. The earlier difference-Fourier maps obtained for $[Ru([12]aneS_4)(bpy)]Cl_2 \cdot 4H_2O$ showed the Cl^- anions disordered over two positions in the crystal structure. Consequently, the coordinates of a Cl^- ion (the asymmetric unit comprises half a cation, one Cl^- and two water molecules) were included in the refinement, occupying two alternative positions with refined occupancies of 51 and 49%, respectively.

The methylenic and aromatic hydrogens were included in the refinement in geometric positions. The hydrogen atoms of water molecules in all three coordination compounds were not found in the final Fourier maps and, therefore, were not included in the corresponding refinements. The structures were refined by least-squares methods until convergence was achieved. The final refinements were made on F^2 using a weighting scheme with the form, $w = 1/[\sigma^2(F_0^2) + (aP)^2 + bP]$, $P = [\max(F_0^2) + 2F_0^2]/3$. The values of parameters a and b are given in Table 1. All calculations required to solve and refine the structures were carried out with SHELXS86 [20] and SHELX93 [21]. The molecular diagrams were drawn with ORTEPII [22]. Additional material is available from the Cambridge Crystallographic Data Centre and comprises atomic coordinates, thermal parameters and the remaining bond lengths and angles.

NMR spectroscopy

All spectra were recorded on a Bruker AMX spectrometer operating at 300 MHz. The ^1H spectra were obtained using 16 K data points and a sweep width of 14.04 ppm. Deuterated methanol was used as a solvent with chemical shifts being referenced to CD_2HOD (3.35 ppm). ^{13}C spectra were recorded using a sweep width of 250 ppm with 32 K data points. Full proton decoupling was used. The deuterated solvent was used as a chemical shift reference (49.0 ppm).

RESULTS AND DISCUSSION

The $[Ru[12]aneS_4(X)]^{2+}$ complexes (X = bpy, phen and dip) were prepared *via* a straightforward process involving only two steps. The first step, the synthesis of the complexes from $[Ru(DMSO)_4Cl_2]$, involved the exchange of the DMSO ligands with the [12]aneS$_4$. Due to the stabilizing effect of the macrocycle ligand this was carried out under mild conditions (reflux at 80°C in EtOH under air) with high yield. The second step was also an exchange reaction, the polypyridyl ligands substituting the chlorides. Again a high yield was obtained using similar conditions.

The single-crystal X-ray diffraction studies of complexes $[Ru([12]aneS_4)(bpy)]Cl_2 \cdot 4H_2O$ (**1**), $[Ru([12]aneS_4)(phen)]Cl_4 \cdot 4.25H_2O$ (**2**), and $[Ru([12]aneS_4)(dip)]Cl_2 \cdot 2H_2O$ (**3**) show hexa-coordination for the Ru centres. Molecular diagrams with their corresponding atomic labeling schemes are shown in Figs 1(a), (b) and (c) for the complex cations $[Ru([12]aneS_4)(bpy)]^{2+}$, $[Ru([12]aneS_4)(phen)]^{2+}$ and $[Ru([12]aneS_4)(dip)]^{2+}$, respectively. Selected bond lengths and angles are listed in Table 2. The cation $[Ru([12]aneS_4)(bpy)]^{2+}$ lies on a two-fold crystallographic axis, making an angle of 29.1(1)° with the plane N(1), N(1′), S(1), S(1′). The structural parameters associated with the Ru coordination sphere indicate a distorted octahedral geometry. The equatorial planes are formed by two sulfur donor atoms from the macrocyclic ligand and two nitrogen atoms from the polypyridyl ligands (bpy, phen or dip). Hexa-coordination is accomplished *via* the remaining two *sulfur* macrocyclic atoms. In each complex, to achieve this geometry, the macrocycle has a considerable fold along the line defined by the axial sulfur donor atoms leading to dihedral angles between the planes S(4),

Table 1. Crystal data and details of structure refinement for $[Ru([12]aneS_4)X]Cl_2 \cdot nH_2O$

Compound	bpy (**1**)	phen (**2**)	dip (**3**)
Molecular formula	$C_{18}H_{32}Cl_2N_2O_4RuS_4$	$C_{20}H_{32.5}Cl_2N_2O_{4.25}RuS_4$	$C_{32}H_{36}Cl_2N_2O_2RuS_4$
M	640.67	669.19	780.84
Crystal system	Monoclinic	Monoclinic	Monoclinic
Space group	$C2/c$	$P2_1/c$	$P2_1/n$
a (Å)	18.127(17)	8.081(9)	11.138(11)
b (Å)	13.004(10)	10.676(9)	9.860(9)
c (Å)	13.343(10)	32.099(28)	30.899(28)
β (°)	99.04(1)	93.54(1)	93.79(1)
U (Å^3)	3106.2	2764.0	3385.9
Z	4	4	4
D_c (g cm^{-3})	1.370	1.608	1.532
μ(Mo-K_α) (mm^{-1})	0.968	1.093	0.900
F(000)	1312	1370	1600
θ range for data collection (°)	1.9–25.1	2.3–25.0	1.9–25.2
Index ranges	$0 \leqslant h \leqslant 21$, $-15 \leqslant k \leqslant 15$, $-15 \leqslant l \leqslant 14$	$0 \leqslant h \leqslant 9$, $-12 \leqslant k \leqslant 12$, $-37 \leqslant l \leqslant 37$	$-13 \leqslant h \leqslant 13$, $0 \leqslant k \leqslant 11$, $-36 \leqslant l \leqslant 36$
Measured reflections	3849	6916	8460
Independent reflections (R_{int})	2369 (0.0316)	4198 (0.0321)	5172 (0.1010)
Data parameters	2364,159	4193,303	5162,389
a and b in weighting scheme	0.1673, 24.84	0.0520, 38.40	0.1700, 19.71
GOF on F^2	1.021	1.099	1.163
R and R_w [$I > 2\sigma(I)$]	0.0772, 0.2241	0.0617, 0.1638	0.1114, 0.2942
R and R_w (all data)	0.0871, 0.2415	0.0681, 0.1696	0.1532, 0.3280
Largest difference peak and hole (e Å^{-3})	0.876, −1.315	0.899, −0.920	0.865, −1.528

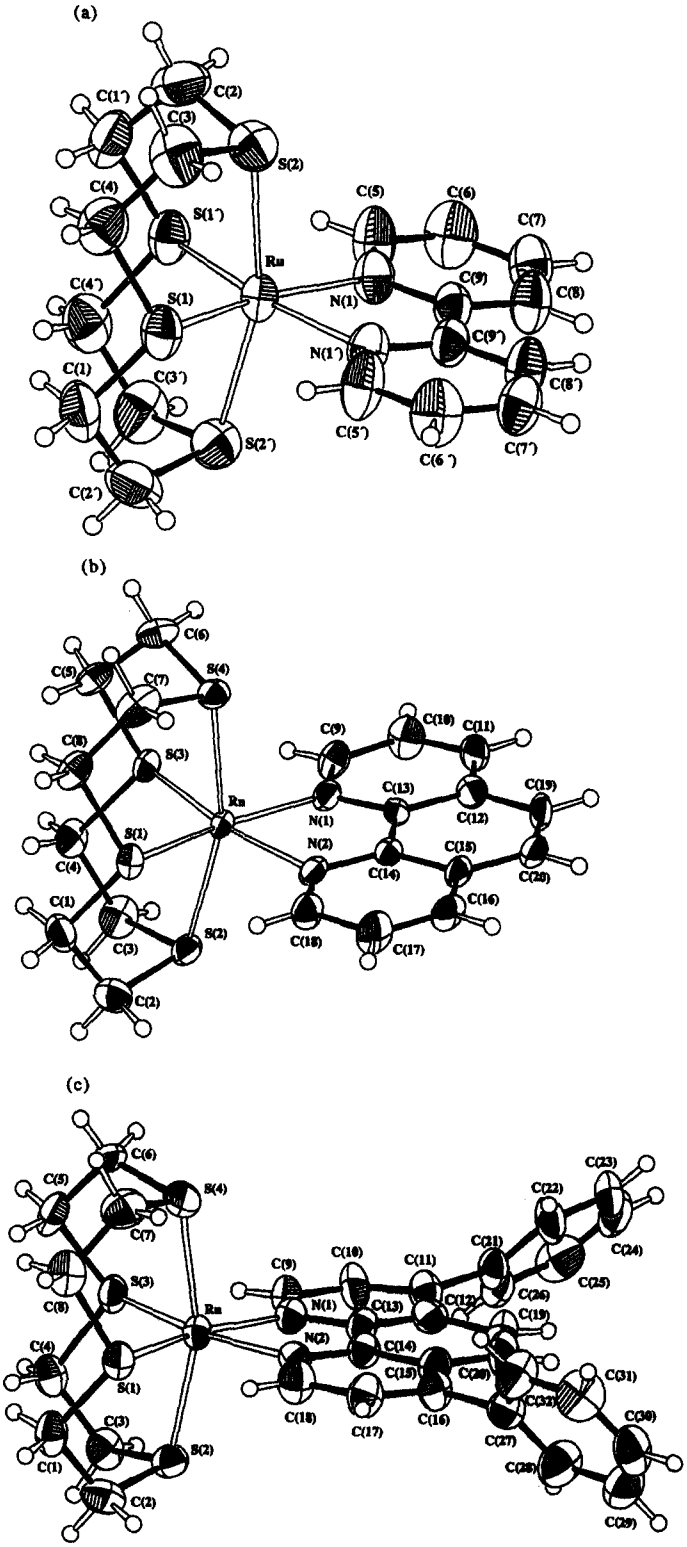

Fig. 1. (a) Molecular structure of the $[Ru([12]aneS_4)(bpy)]^{2+}$ complex cation showing the atomic labelling scheme (thermal ellipsoids 50%). (b) Molecular structure of the $[Ru([12]aneS_4)(phen)]^{2+}$ complex cation showing the atomic labelling scheme (thermal ellipsoids 50%). (c) Molecular structure of the $[Ru([12]aneS_4)(dip)]^{2+}$ (thermal ellipsoids 50%).

Table 2. Selected bond lengths (Å) and angles (°) for Ru coordination sphere of complexes **1**, **2** and **3**

	bpy (**1**) [$x, y = 1'; z = 2'$]	phen (**2**) [$x = 2; y = 3; z = 4$]	dip (**3**) [$x = 2; y = 3; z = 4$]
Ru—N(1)	2.162(6)	2.162(7)	2.134(10)
Ru—N(2)		2.156(6)	2.138(9)
Ru—S(1)	2.309(2)	2.319(2)	2.318(3)
Ru—S(3)		2.313(2)	2.323(3)
Ru—S(2)	2.420(2)	2.397(2)	2.385(3)
Ru—S(4)		2.384(2)	2.408(3)
N(1)—Ru—N(x)	77.9(3)	79.6(3)	77.4(4)
N(1)—Ru—S(1)	166.7(2)	166.6(2)	166.6(3)
N(2)—Ru—S(3)		167.5(2)	166.5(2)
N(1)—Ru—S(y)	88.8(2)	88.0(2)	89.2(3)
N(2)—Ru—S(1)		87.3(2)	89.3(2)
S(1)—Ru—S(y)	104.5(1)	105.1(1)	104.1(1)
S(2)—Ru—S(z)	162.5(2)	161.9(1)	162.0(1)
S(3)—Ru—S(4)		84.9(1)	83.8(1)
N(2)—Ru—S(4)		95.1(2)	98.0(3)
N(1)—Ru—S(z)	97.4(2)	93.9(2)	93.8(2)
N(1)—Ru—S(2)	96.2(2)	99.9(2)	95.9(3)
N(2)—Ru—S(2)		98.8(2)	98.0(3)
S(1)—Ru—S(2)	84.9(1)	84.6(1)	84.3(1)
S(3)—Ru—S(2)		83.9(1)	85.0(1)
S(1)—Ru—S(z)	84.4(1)	84.6(1)	84.8(1)

S(2), S(3) and S(4), S(2), S(1) of 58.6(1)° and 59.8(1)° in complexes **2** and **3**, respectively. The dihedral angle between the planes S(1), S(2), S(2′) and S(1′), S(2), S(2′) is 59.4(8)° in complex **1**.

In all three complexes, the angle between axial sulfur donor atoms and Ru centre (S_{ax}—Ru—S_{ax}) is much smaller than the expected 180° for an ideal octahedral [S(2)—Ru—S(4) 161.9(1)° phen, 162.0(1)° dip and S(2)—Ru—S(2′) 162.5(2)° bpy]. This contrasts with the situation observed for octahedral complexes containing nine-, 14- or 18-membered polythiamacrocyclic ligands. In the complexes [Ru([12]aneS_4)Cl_2] ([14]aneS_4 = 1,4,8,11- tetrathiacyclotetradecane) [23] and [Ru([12]aneS_4)Cl(PPh_3)]$^+$ [24] the angles S_{ax}—Ru—S_{ax} are 174.9 and 175.8°, respectively, while in the complexes [Ru([18]aneS_6)]$^{2+}$ ([18]aneS_6 = 1,4,7,10,13,16-hexathiacyclooctadecane)] and [Ru([9]aneS_3)$_2$]$^{2+}$ with two [9]aneS_3 ([9]aneS_3 = 1,4,7-trithiacyclononane) units the Ru centre has a crystallographic inversion centre and the angle S_{ax}—Ru—S_{ax} is exactly 180° [25]. This structural feature reflects the small cavity size of the [12]aneS_4 ligand when accommodating the Ru centre in a *cis*-octahedral environment. In metal complexes of nine-, 14- and 18-membered macrocyles there is a good size match between the Ru centre and the available cavity of these macrocyclic ligands.

The axial Ru—S bond lengths [Ru—S_{ax} = 2.420(2) bpy, 2.384(2) and 2.397(2) phen and 2.385(3) and 2.408(3) Å dip] are significantly longer than the equatorial Ru—S distances [Ru—S_{eq} = 2.309(2) bpy, 2.313(2) and 2.319 phen and 2.318(3) and 2.323(3) Å dip] in all three complexes. In contrast the complexes [Ru([18]aneS_4)]$^{2+}$ [Ru—S_{ax} = 2.339(2) and Ru—S_{eq} = 2.334(2) Å] and [Ru([9]aneS_3)$_2$]$^{2+}$ [Ru—S_{ax} = 2.322(2) and Ru—S_{eq} = 2.337(2) Å] have axial distances which are similar to the equatorial distances. This comparison suggests that the small cavity size [12]aneS_4 also plays an important role in determining the Ru—S_{ax} bond lengths.

The average Ru—S_{eq} bond lengths [2.309(2) bpy, 2.316(2) phen and 2.320(3) Å dip] are similar to those observed for the complexes [Ru([9]aneS_3)(phen)Cl]$^+$ 2.288(2) and [Ru([9]aneS_3)(bpy)Cl]$^+$ 2.318(2) Å [26].

The angles in the equatorial plane involving the nitrogen atoms and metal centre differ from ideal octahedral values due to the small bite angles of polypyridyl ligands [77.9(3) bpy, 79.6(3) phen, and 77.4(4)° dip]. These values are similar to those seen for the octahedral complexes [Ru([9]aneS_3)(phen)Cl]$^+$ 78.4(3), [Ru([9]aneS_3)(bpy)Cl]$^+$ 77.8(2) [Ru(bpy)(NO)Cl_2F], 79.4(2), [Ru(bpy)$(CO)_2Br_2$] 77.2(3), [Ru(bpy)$(CO)_2I_2$] 76.3(5), [Ru_2(bpy)$_2Br_5(H_2O)$] 79.0(4) and 78.5(4)° [27].

The average Ru—N bond distances observed for three complexes [2.162(6) bpy, 2.159(7) phen and 2.136(5) Å dip] are longer than those found for related complexes containing phen or bpy ligands: [Ru([9]aneS_3)(bpy)Cl]$^+$ 2.108(5), [Ru([9]aneS_3)(phen)Cl]$^+$ 2.083(6), [Ru(bpy)(NO)Cl_2F] 2.079(6), [Ru(bpy)$(CO)_2Br_2$] 2.117(9), [Ru(bpy)$(CO)_2I_2$] 2.116(12) Å and binuclear complex [Ru_2(bpy)$_2$ $Br_5(H_2O)$] 2.071(9) and 2.075(10) Å.

The bpy ligand in complex **1** is not absolutely

planar, leading to an angle between the pyridine rings of 5.1(4)°, which is reduced to 2.8(5) and 3.2(6)° for phen and dip complexes, respectively. The phen and dip ligands are more resistant to deformation from overall planar geometry than the bpy, as would be expected.

A search of the Cambridge Database [28] revealed only two other complexes containing the [12]aneS$_4$ ligand in octahedral coordination environments: [Rh([12]aneS$_4$)(phi)]$^{3+}$ (phi = 9,10-phenanthrenequinonediamine) [17] and [Ni$_2$([12]aneS$_4$)$_2$Cl$_2$], where two [Ni([12]aneS$_4$)]$^{2+}$ units are linked by two chlorine bridges [29]. A comparison of the endocyclic S—C—C—S, C—C—S—C and C—S—C—C torsion angles for these complexes and the Ru complexes are shown in Table 3. This comparison indicates that the macrocycle adopts two different conformations: one for the three Ru complexes and another for the Rh and Ni complexes. These conformations are illustrated in Fig. 2 for complexes [Ru([12]aneS$_4$)(phen)Cl]$^{2+}$ and [Rh([12]aneS$_4$)(phi)]$^{3+}$. The macrocycle in the phen and dip complexes has a symmetric conformation with the two S—CH$_2$—CH$_2$—S—CH$_2$—CH$_2$—S moieties related by an approximate twofold axis bisecting the N-•-Ru—N angle. The bpy complex has C_2 symmetry imposed crystallographically. In the Ni and Rh complexes the two S—CH$_2$—CH$_2$—S—CH$_2$—CH$_2$—S moieties are related by a single mirror plane.

In a conformational analysis of the free [12]aneS$_4$ ligand in the gas phase [30], the two conformations observed in the Ru and Rh and Ni complexes were found to differ in energy by only 5.1 kJ mol^{-1}. This result shows that either of these conformations can be adopted by the [12]aneS$_4$ in *cis*-octahedral environment. The molecular modelling of these type of [12]aneS$_4$ complexes is in progress.

All the ^{1}H and ^{13}C spectra for the three complexes indicate that the stoichiometry is as expected. The ^{1}H NMR spectrum of the aromatic regions of the complexes [Ru([12]aneS$_4$)(phen)]$^{2+}$, [Ru([12]aneS$_4$)(bpy)]$^{2+}$ and [Ru([12]aneS$_4$)(dip)]$^{2+}$ are shown in Fig. 3. It can be seen that all the complexes display broad lines for the H2/H9 protons of the phen and dip ligands and for the H6/6′ protons of the bpy ligand. The broad peaks integrate to two protons as expected. These broad lines suggest that chemical exchange is taking place in solution. The ^{13}C spectra for all the complexes also show broad lines for the C2/C9 carbons in phen and dip and for the C6/6′ carbons in bpy. The CH$_2$ carbons of the [12]aneS$_4$ ligand display broad lines with the higher field peak broader than the other. Both peaks integrate to the same area.

In order to confirm that exchange was occurring a variable temperature study was carried out. ^{1}H spectra for all three complexes in CD$_3$OD at 5, 10, 23, 30, 40 and 50°C were recorded and the regions containing the phen and dip H2/H9 and bpy H6/6′ peaks are shown in Fig. 4. As the temperature is increased from 5 to 50°C the peaks can be seen to go from a doublet

Table 3. Two different folded conformations of [12]aneS$_4$ characterized by the torsion angles listed successively along the ring at the S—C—C—S angle

Compound	Torsion angles (°)											Ref.
[Ru([12]aneS$_4$)(bpy)]$^{2+}$	−51.9(9)	−76.4(8)	74.7(8)	52.0(8)	−164.7(6)	165.7(6)	−51.9(9)	−76.4(8)	74.7(8)	52.0(8)	−164.7(6)	−165.7(6)	This work
[Ru([12]aneS$_4$)(phen)]$^{2+}$	−51.7(8)	−74.7(8)	78.9(8)	50.1(9)	−166.5(6)	163.2(6)	−52.0(8)	−74.6(7)	78.6(7)	50.1(8)	−166.1(6)	163.2(6)	This work
[Ru([12]aneS$_4$)(dip)]$^{2+}$	−50.6(10)	−79.2(10)	75.2(10)	50.2(10)	−160.5(8)	166.6(8)	−49.4(10)	−79.5(10)	73.7(11)	50.5(12)	−162.0(8)	166.9(8)	This work
[Rh([12]aneS$_4$)(phi)]$^{3+}$	−54.2	123.4	−74.1	−58.1	161.8	−159.9	55.3	78.0	−124.5	54.5	−164.8	163.4	[17]
[Ni$_2$([12]aneS$_4$)$_2$Cl$_2$]	−59.0	125.1	−75.1	−60.7	157.9	−157.9	60.7	75.1	−125.1	59.0	−163.2	163.2	[29]

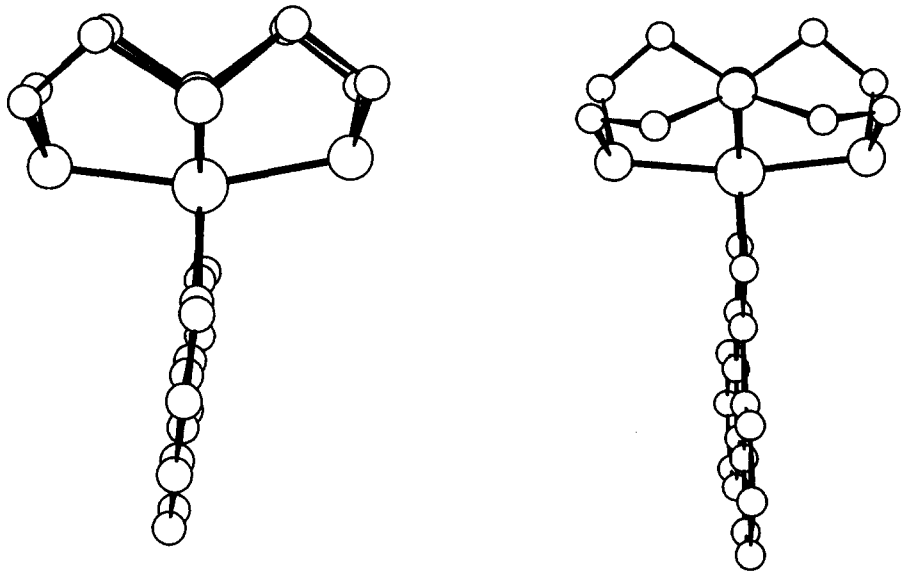

$[Ru([12]aneS_4)(phen)]^{2+}$ $[Rh([12]aneS_4)(phi)]^{3+}$

Fig. 2. A comparison of the two different [12]aneS$_4$ macrocycle conformations adopted in $[Ru([12]aneS_4)(phen)]^{2+}$ and $[Rh([12]aneS_4)(phi)]^{3+}$

through a broad singlet to a doublet again. At ambient temperatures the observed broad peak is therefore a result of exchange between two sites. The [12]aneS$_4$ peaks exhibit similar although less pronounced changes. At 5 and 50°C the peaks exhibit some structure while at room temperature the lines are broad and featureless.

From the NMR data it is possible, in principle, to obtain kinetic information about the rate of the exchange process and also about the populations of the two states [31]. If the low and high temperature spectra can be assumed to be the two extremes, i.e. fully "bound" and fully unbound or "free" then the position of the NMR peak can be related to the population of the two states and the width of the NMR lines can be related to the rate of exchange between the two states. However, the situation is not so simple as factors such as the change of chemical shift of the NMR lines and transverse relaxation rates with temperature also have an effect on calculated rates and populations. It must also be remembered that although NMR can give information about the kinetics of the exchange between the two situations, no mechanistic information can be directly obtained. The variation of the chemical shift and linewidth encountered for these complexes suggests that the population and rate of exchange are both varying with temperature.

The values for ν_B (chemical shift of the "bound" form) and ν_F (chemical shift of the "free" form) can be estimated, however, using plots of chemical shift versus temperature. From these plots ν_B for bpy, phen and dip were estimated to be 2565, 2662 and 2690 Hz, respectively. The ν_F values were 2525, 2625 and 2650 Hz. By plotting $(\nu_{exp}-\nu_F)/(\nu_F-\nu_B)$ versus temperature an estimation of the variation of population of the "bound" and "free" states can be obtained. Figure 5 shows the variation of these states for all three complexes. It can be seen that the phen and dip complexes exhibit very similar behaviour, i.e. a bound-free crossing point at ca. 303 K, while the bpy complex shows a crossing point at ca. 293 K.

From X-ray studies in the solid state the complexes display distorted octahedral geometry due to the small bite angle of the polypyridyl ligands and the constraints of the macrocycle. In solution this strain may be alleviated by either a Ru—N or Ru—S bond being broken and the vacant site may be taken, temporarily, by the solvent. Exchange may therefore be occurring between a situation with all S and N atoms of the polypyridyl and [12]aneS$_4$ ligands bound and a situation where one S of the macrocycle or one N of the polypyridyl is unbound. If the exchange process between the two forms of the complexes involves one of the polypyridyl nitrogens becoming unbound then we may expect a difference to be observed between the phenanthroline type ligands and the bpy ligand as the phen type ligands are planar while the bpy ligand has freedom of rotation about its 2,2′ bond. Therefore, once unbound, the bpy ligand has more degrees of freedom and may therefore explain the exchange midpoint being at a lower temperature than the phen type ligands. This suggests that a Ru—N bond is being broken rather than a Ru—S bond.

By measuring the linewidth of the NMR peak at the 50/50 situation it is possible to calculate [31] the

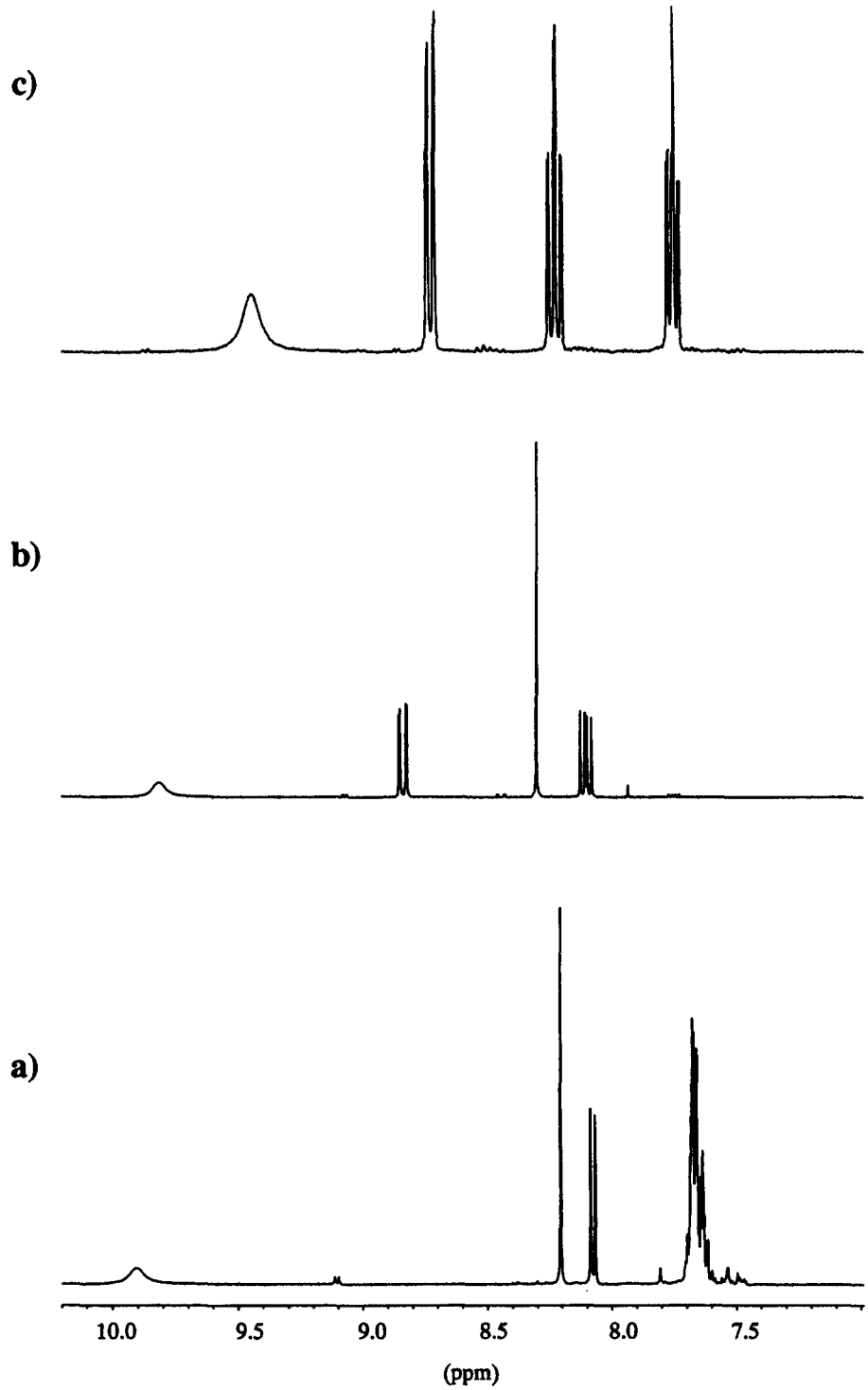

Fig. 3. ^{1}H NMR spectrum of the aromatic regions of (a) $[Ru([12]aneS_4)(dip)]^{2+}$, (b) $[Ru([12]aneS_4)(phen)]^{2+}$ and (c) $[Ru([12]aneS_4)(bpy)]^{2+}$ in CD_3OD.

rate of exchange (at that temperature) using $\Delta\nu_{1/2} = 1/2\pi(\nu_B - \nu_F)^2 k^{-1}$. The rate constant can then be used to obtain $\Delta G\ddagger$, the free energy of activation of the process *via* $k_r = \kappa(kT/h)\exp(-\Delta G\ddagger/RT)$ where k_r is the rate of exchange and κ is an activation constant usually taken as 1. For complexes **1**, **2** and **3** the values for $\Delta\nu_{1/2}$ are 25.8, 19.8 and 21.2, respectively. From these estimations assuming an error of 1 Hz for $\Delta\nu_{1/2}$ and 2 Hz for $\nu_B - \nu_F$ the $\Delta G\ddagger$ values for the exchange processes are 66.1 ± 0.4, 68.2 ± 0.4 and 68.0 ± 0.4 kJ mol^{-1} for complexes **1**, **2** and **3**, respectively. These results suggests the phen and dip com-

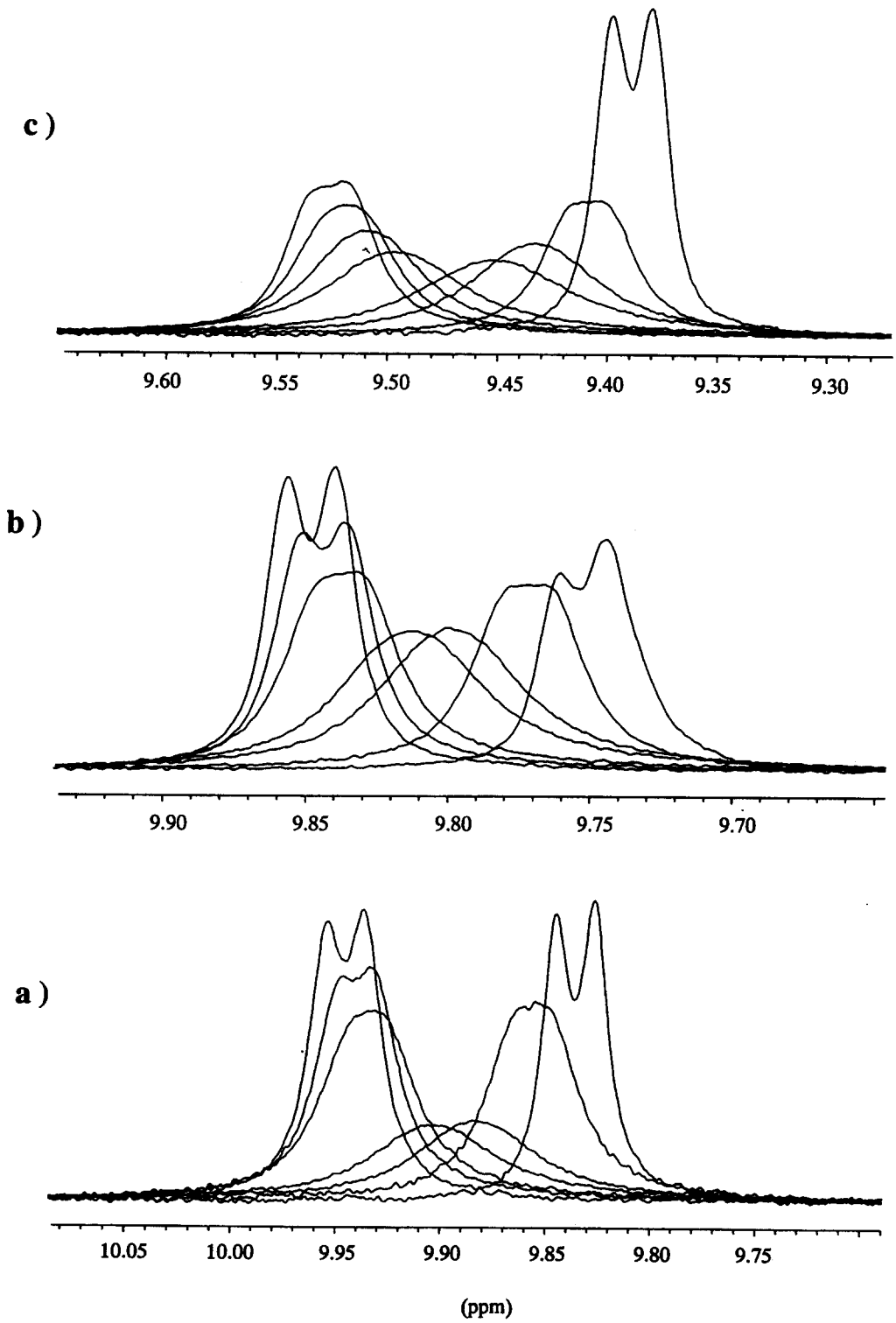

Fig. 4. Variable-temperature ^{1}H NMR spectra of the H2/H9 protons of (a) [Ru([12]aneS$_4$)(dip)]$^{2+}$, (b) [Ru([12]aneS$_4$)(phen)]$^{2+}$ and (c) the H6/6′ protons of [Ru([12]aneS$_4$)(bpy)]$^{2+}$. Spectra were recorded at 323, 313, 303, 298, 288, 283 and 278 K in CD_3OD. All the resonances for the three complexes shift to low field with decreasing temperature.

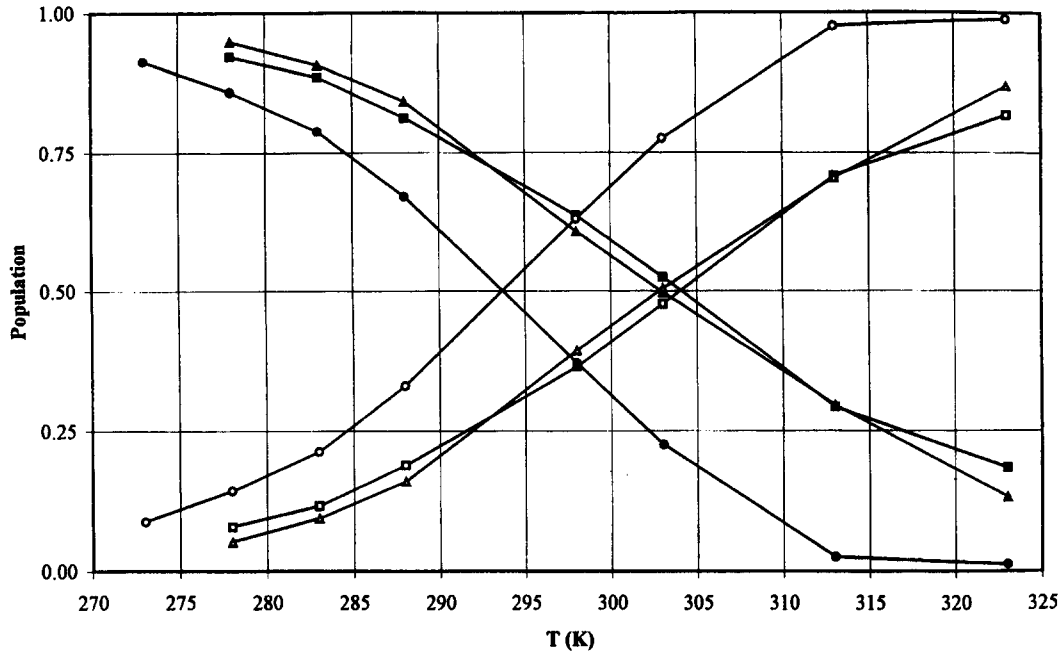

Fig. 5. A plot of the estimated variation of the populations of the "bound" and "free" states for $[Ru([12]aneS_4)(bpy)]^{2+}$ (the open circles and closed circles represent the "free" and "bound" populations) $[Ru([12]aneS_4)(phen)]^{2+}$ (open and closed squares) and $[Ru([12]aneS_4)(dip)]^{2+}$ (open and closed triangles).

plexes have similar free energies of activation, while the bpy complex has a slightly lower free energy. The fact the values are similar suggests the same process is occurring for the three complexes.

Acknowledgements—We thank the EPSRC and the University of Reading for the image plate system and Johnson Matthey for the loan of $RuCl_3$. We also thank Mr A. W. Johans for his technical assistance with the crystallographic studies and Dr A. M. S. Silva and H. Tavares for assistance with the variable-temperature NMR. V. F. acknowledges the Junta Nacional de Investigação Cientifica e Tecnológica, the Fundação Gulbenkian and the British Council for travel grants.

REFERENCES

1. Barton, J. K. and Lolis, E., *J. Am. Chem. Soc.*, 1985, **107,** 708.
2. Kumar, C. V., Barton, J. K. and Turro, N. J., *J. Am. Chem. Soc.*, 1985, **107,** 5518.
3. Barton, J. K., *Science*, 1986, **233,** 727.
4. Barton, J. K., Goldberg, J. M., Kumar, C. V. and Turro, N. J., *J. Am. Chem. Soc.*, 1986, **108,** 2081.
5. Pyle, A. M., Rehmann, J. P., Kumar, C. V., Turro, N. J. and Barton, J. K., *J. Am. Chem. Soc.*, 1989, **111,** 3051.
6. Pyle, A. M. and Barton, J. K., *Prog. Inorg. Chem.*: *Bioinorg. Chem.*, 1990, **38,** 413.
7. Hiort, C., Norden, B. and Rodger, A., *J. Am. Chem. Soc.*, 1990, **112,** 1971.
8. Rehmann, J. P. and Barton, J. K., *Biochem.*, 1990, **29,** 1710.
9. Eriksson, M., Leijon, M., Hiort, C., Norden, B. and Graslund, A., *J. Am. Chem. Soc.*, 1992, **114,** 4933.
10. David, S. S. and Barton, J. K., *J. Am. Chem. Soc.*, 1993, **115,** 2984.
11. Tysoe, S. A., Morgan, R. J., Baker, A. D. and Strekas, T. C., *J. Phys. Chem.*, 1993, **97,** 1707.
12. Naing, K., Takahashi, M., Taniguchi, M. and Yamagishi, A., *Inorg. Chem.*, 1995, **34,** 350.
13. Rosenberg, B., Van Camp, L., Trosko, J. E. and Mansour, V., *Nature*, 1969, **222,** 385.
14. Alessio, E., Mestroni, G., Nardin, G., Attia, W. M., Calligaris, M., Sava, G. and Zoret, S., *Inorg. Chem.*, 1988, **27,** 4099.
15. Keppler, B. K., Henn, M., Juhl, U. M., Berger, M. R., Niebl, R. and Wagner, F. E., *Prog. Clin. Biochem.*, 1989, **10,** 41.
16. Cooper, S. R., Rawle, S. C., Yagbasan, R. and Watkin, D. J., *J. Am. Chem. Soc.*, 1991, **113,** 1600.
17. Krotz, A. H., Kuo, L. Y. and Barton, J. K., *Inorg. Chem.*, 1993, **32,** 5963.
18. Evans, I. P., Spencer, A. and Wilkinson, G., *J. Chem. Soc., Dalton Trans.*, 1973, 204.
19. Kabsch, W., *J. Appl. Cryst.*, 1988, **21,** 916.
20. Sheldrick, G. M., in *Crystallographic Computing* 3, ed. G. M. Sheldrick, G. M. Sheldrick, C. Krüger and R. Goddard. Oxford University Press, Oxford, 1985.
21. Sheldrick, G. M., University of Göttingen, Germany, 1994.
22. Johnson, C. K., *ORTEP*II, *A Fortran Thermal-Ellipsoid Plot Program for Crystal Structure Illustrations.* Report ORNL-5138, Oak Ridge National Laboratory, Oak Ridge, Tennessee, 1976.

23. Lai, T.-F. and Poon, C.-K., *J. Chem. Soc., Dalton Trans.*, 1982, 1465.
24. Alcock, N. W., Cannadine, J. C., Clark, G. R. and Hill, A. F., *J. Chem. Soc., Dalton Trans.*, 1993, 1131.
25. Bell, M. N., Blake, A. J., Holder, A. J., Hyde, T. I. and Schröder, M., *J. Chem. Soc., Dalton Trans.*, 1990, 3841.
26. Goodfellow, B. J., Félix, V., Pacheco, M. D., Pedrosa de Jesus, J. and Drew, M. G. B., *Polyhedron*, 1997, **16**, 393.
27. Haukka, M., Algrén, M. and Pakkanen, T. A., *J. Chem. Soc., Dalton Trans.*, 1996, 1927.
28. Allen, F. H., Davies, J. E., Galloy, J. J., Johnson, O., Kennard, O., Macrae, C. F. and Watson, D. G., *J. Chem. Inf. Comput. Sci.*, 1991, **31**, 204.
29. Blacke, A. J., Halcrow, M. A. and Schröder, M., *J. Chem. Soc., Dalton Trans.*, 1994, 1463.
30. Drew, M. G. B. and Félix, V., unpublished results.
31. Harris, R. K., *Nuclear Magnetic Resonance Spectroscopy*. Longman, Harlow, U.K., 1986.